Journal of Hazardous Materials 408 (2021) 124453

Contents lists available at ScienceDirect

Journal of Hazardous Materials

journal homepage: www.elsevier.com/locate/jhazmat

Research paper

Bioaccumulation kinetics and internal distribution of the fission products radiocaesium and radiostrontium in an estuarine crab

Tom Cresswell [a,*], Emily Prentice [a,b], Nick Howell [a], Paul Callaghan [a], Marc Metian [c], Mathew P. Johansen [a]

[a] ANSTO, Locked Bag 2001, Kirrawee DC, NSW 2232, Australia
[b] NSW Office of Environment and Heritage, PO Box 29, Lidcombe, NSW 1825, Australia
[c] International Atomic Energy Agency Environment Laboratories (IAEA-EL), Radioecology Laboratory, 4a Quai Antoine 1er, Principality of Monaco MC-98000, Monaco

ARTICLE INFO

Editor: Dr. R Teresa

Keywords:
Radionuclides
Invertebrates
Biokinetics
Organ distribution
Moulting

ABSTRACT

Crab has been designated by the ICRP as one of twelve reference/model organisms for understanding the impacts of radionuclide releases on the biosphere. However, radionuclide-crab interaction data are sparse compared with other reference organisms (e.g. deer, earthworm). This study used an estuarine crab (*Paragrapsus laevis*) to investigate the contribution of water, diet and sediment sources to radionuclide (^{134}Cs and ^{85}Sr) bioaccumulation kinetics using live-animal radiotracing. The distribution of each radionuclide within the crab tissues was determined using dissection, whole-body autoradiography and synchrotron X-ray Fluorescence Microscopy (XFM). When moulting occurred during exposure, it caused significant increases in ^{85}Sr bioaccumulation and efflux of ^{134}Cs under constant aqueous exposure. Dietary assimilation efficiencies were determined as 55 ± 1% for ^{134}Cs and 49 ± 3% for ^{85}Sr. ^{85}Sr concentrated in gonads more than other organs, resulting in proportionally greater radiation dose to the reproductive organs and requires further investigation. ^{134}Cs was found in most soft tissues and was closely associated with S and K. Biodynamic modelling suggested that diet accounted for 90–97% of whole-body ^{137}Cs, while water accounted for 59–81% of ^{90}Sr. Our new data on crab, as a representative invertebrate, improves understanding of the impacts of planned or accidental releases of fission radionuclides on marine ecology.

1. Introduction

The operation of nuclear facilities results in the production of the radiocaesium (^{137}Cs) and radiostrontium (^{90}Sr), among other radionuclides, as a consequence of uranium fission. These products have the potential to enter the aquatic environment, especially following accidents at nuclear facilities such as occurred at the Fukushima Daiichi Nuclear Power Plant (FDNPP), Japan, following the tsunami caused by the Tōhoku earthquake on 11 March 2011. As both isotopes have half-lives of approximately 30 years, these radionuclides are persistent in the environment and inevitably are taken up into the biota inhabiting marine systems. In the months after the accident, ^{137}Cs and ^{90}Sr activity concentrations in seawater < 10 km of the FDNPP were respectively 6 and 3 orders of magnitude above pre-accident levels (>1000 Bq/L and >1 Bq/L respectively; Supporting information Table 1; Nuclear Regulatory Agency, Japan, http://radioactivity.nsr.go.jp). Similarly, ^{137}Cs and ^{90}Sr surface sediment concentrations were determined to be > 1000 and > 10 Bq/kg dry weight (dw) respectively between 2011 and 2012 (Supporting information Table 1; Kusakabe et al., 2013).

The partition coefficients (k_d) for both radionuclides are moderate in marine sediments at 1–4000 and 1–200 L/kg for Cs and Sr respectively (IAEA, 2004; Takata et al., 2014) and > 10,000 L/kg for Cs in estuarine conditions (geometric mean; Johansen et al., 2019). As both radionuclides have an affinity to adsorb to sediments, benthic communities will more likely be exposed than the pelagic. Post-accident studies at Fukushima have shown ^{134,137}Cs were highest in demersal fish species with sediment-associated food chains (Wada et al., 2016; Fiévet et al., 2017; Takata et al., 2019). Several papers have commented on the sparse data for radionuclides that are more difficult to measure, such as ^{90}Sr, in organisms affected by the FDNPP and an absence of information on the specific organ distribution of Cs and Sr radionuclides in field organisms (Castrillejo et al., 2016; Buesseler et al., 2017). The lack of data for ^{90}Sr is important to highlight given its substantial beta emissions at 546 and 2284 keV (both at 100% incidence), which could result in significant

* Corresponding author.
E-mail address: tom.cresswell@ansto.gov.au (T. Cresswell).

https://doi.org/10.1016/j.jhazmat.2020.124453
Received 2 September 2020; Received in revised form 22 October 2020; Accepted 30 October 2020
Available online 2 November 2020

internal radiological doses to organisms.

Once accumulated into aquatic organisms, Cs predominantly tends to accumulate in the muscle tissue of vertebrates and invertebrates (Metian et al., 2016; Pouil et al., 2018), although it is species specific (Metian et al., 2016). In parallel, many studies have suggested Cs has the potential to biomagnify with increasing trophic levels in aquatic food webs (Kasamatsu and Ishikawa, 1997; Zhao et al., 2001; Mathews and Fisher, 2008; Pan and Wang, 2016; Pouil et al., 2018). Bioaccumulated Sr tends to accumulate in hard (e.g. shell), rather than the soft tissues such as gills or digestive tissues (e.g. up to a factor of 40 in the bones of fish; Lee et al., 2013; Johansen et al., 2015).

The accumulation of radiocaesium in marine organisms becomes important for humans when seafood is consumed. Concern over this dose pathway lead to fishing restrictions and subsequent economic impacts following the FDNPP accident. Five years after the accident, all of the fish sampled within 20 km of the FDNPP demonstrated a decreasing trend of radiocaesium concentrations, while only a few fish gathered near the FDNPP still exceeded consumption standards (Japanese regulatory limit of 100 Bq/kg; Wada et al., 2016). Bioaccumulated radiocaesium is important for the dose to the organisms themselves, as the mass and volume of the muscle are typically relatively large and therefore contribute higher dose rates than other tissues. Similarly for radiostrontium, after accumulation in bone or exoskeleton, the beta emissions deposit their energy in nearby tissues (within approximately 10 mm) resulting in nearly all its ionising dose being absorbed by the host organism (Johansen et al., 2015). For ^{134,137}Cs, these dose rates can potentially magnify through food chains (with potential biomagnification of the associated element; Rowan and Rasmussen, 1994). Therefore it is prudent to understand biological uptake in crustaceans which are ubiquitous in ecosystems and often fill a foundation role in food chains. Furthermore, the International Commission on Radiological Protection (ICRP) has identified the crab as an aquatic invertebrate reference species for radiological dosimetry (ICRP, 2008).

This study aimed to characterise the bioaccumulation of radiocesium and radiostrontium in a decapod crustacean. We sought to quantify the relative contribution of dietary and water sources to Cs and Sr radionuclide transfer to a decapod crustacean under environmental release scenarios (planned or accidental). We also investigated how the transfer pathway (the uptake of dissolved species via gills or ingestion of dietary-associated radionuclides) affects the in vivo uptake of each radionuclide and its bioaccumulation kinetics. By investigating the predominant sources of each radionuclide and subsequent biokinetic rates and biodistribution, we have provided key data for the risk assessment of radionuclide releases to marine systems. This, in turn, allows for a more robust assessment of the impacts of radionuclides to marine decapod crustaceans, the ecological food chains and their human consumers.

2. Experimental

2.1. Animal collection and holding conditions

Adult male mottled shore crabs (*Paragrapsis laevis*; Dana, 1851; 6.2 ± 1.6 g wet weight (ww), mean ± SD; n = 40) were collected from an estuarine bay (Bonnet Bay) near Sydney, Australia (34° 0′28" S; 151° 2′58" E). Males were selected due to the collection permit restrictions obtained from our local authority. Crabs were collected by hand and transported to Australia's Nuclear Science and Technology Organisation (ANSTO), Lucas Heights, NSW within two hours of collection. Animals were maintained in filtered (< 0.45 μm) estuarine water (15 L in a 60 L tank) collected from the Woronora Estuary with the following conditions: 25 ± 0.5 mg/L salinity (total dissolved solids); 39 ± 1 mS/cm specific conductivity; 7.8 ± 0.1 pH; 21 ± 1 °C water temperature; > 7 mg/L dissolved oxygen (same parameters also apply to all experiments) on a 12 h:12 h light:dark photoperiod. Crabs were fed commercial food pellets (NovoRift, Germany) three times per week and uneaten food/faeces were siphoned with approximately 25% of holding tank water, the day after feeding. This water was replaced with clean estuarine water. For each experiment listed below, crabs of a similar size were removed from the holding tank, weighed fresh and their carapace lengths and widths recorded. The background Cs and Sr concentrations of whole crabs collected from the field were < 200 μg/kg and 1720 ± 353 mg/kg respectively (mean ± SD, n = 3) as determined by acid digestion and subsequent ICP-MS analysis (Varian 820MS Quadrupole; all samples run with internal standard correction for matrix and drift correction).

2.2. Exposure to dissolved radionuclides

To determine bioaccumulation kinetic parameters of dissolved Cs and Sr, crabs were exposed to ^{134}Cs and ^{85}Sr respectively for two weeks using a method of static renewal described by Cresswell et al. (2015). Individual spiking solutions were prepared from stocks of ^{134}Cs (produced at ANSTO, Sydney, Australia in 0.1 M HCl) and ^{85}Sr (Eckert & Zeigler, Valencia, USA; in 0.1 M HCl). Approximately 1.6 mL of each radionuclide spiking solution (100 kBq/mL) was added to separate bottles containing 3.2 L of estuarine water and the bottle shaken to homogenise the solution. The resultant spiked estuarine water (50 kBq/L for each radionuclide) was transferred to eight 1.1 L polyethene containers (400 mL in each) with holes drilled in the lids to allow a soft plastic tube to deliver compressed air to the solution. Subsamples (10 mL) were randomly collected from two containers of each radionuclide treatment and radioanalysed to confirm the exposure activity concentration. One crab was transferred to each of the 16 containers to begin the experiment. The solution activity concentrations used in this exposure were chosen to facilitate a rapid (< 10 min) count time of animals and solution samples. Experimental Cs and Sr additions related to the radiotracer corresponded to 0.96 and 0.86 μg/L (7.2 and 9.8 nmol/L) respectively. These concentrations are comparable to those found in surface sea waters of 0.4–1.3 μg/L (3.0–9.8 nmol/L; Bryan, 1961) for Cs and well below the concentrations of Sr off the coast of Japan 7910 ± 40 μg/L (90 ± 0.5 nmol/L; Nagaya et al., 1971). Non-amended estuarine water used in the experiment was analysed by ICP-MS and showed < 1 and 4635 μg/L (7.5 nmol/L and 52 μmol/L) for Cs and Sr respectively. Natural potassium (K^+) concentration in estuarine water used for animal holding and all experiments was 370 mg/L (9.4 mmol/L). The chemical speciation model WHAM (Tipping, 1994), using estuarine water cation and anion concentrations (as determined via ICP-MS) predicted that 100% of Cs and Sr were present in solution as the mono and divalent ions (i.e. Cs^+ and Sr^{2+}) respectively.

Each crab was radioanalysed alive every 2 h for the first 10 h, daily up to 8 d exposure then every 1–2 days until 14 d exposure. Exposure solutions were renewed 100% every second day and water samples of the exposure solution were collected at random and radioanalysed every day for the first week and every second day for the last week of exposure. Crabs were fed outside the exposure water during radioanalysis every second day (see Section 2.3). Following 14-d exposure, animals were transferred to new individual 1.1 L containers with 400 mL non-active estuarine water and allowed to depurate for 3 weeks. Crabs were radioanalysed every 2–3 days during depuration. The cumulative radiological doses to crabs from exposure to dissolved ^{134}Cs and ^{85}Sr were modelled using the ERICA Tool (v.1.2.1) and compared to international benchmarks for potential effects as described in the Supporting information. The predicted total dose rates of 65 and 18 μGy/h for ^{134}Cs and ^{85}Sr, respectively, over the duration of the exposure, were not expected to adversely impact individuals from a radiological dose perspective.

2.3. Radioisotope detection and live-animal radioanalysis

Water samples (10 mL) to verify exposure activity were radioanalysed in 20 mL plastic liquid scintillation (LSC) vials and compared against in-house standards in the same (standard) geometry prepared with a known activity of the ^{134}Cs and ^{85}Sr sources used in this study

preserved in 0.1 M HCl. The activities of all in-house liquid standards were confirmed with HPGe gamma spectrometry (ORTEC) against standards in the same geometry (Eckert and Ziegler, Germany). Gamma-ray emissions from water and live crab samples were determined using a 1.5 × 1.5" LaBr coaxial detector (63 cm diameter) housed in a lead shield (17 cm internal diameter × 30 cm internal height, 17 cm cylinder thickness with 14 cm thick lid). The detector was attached to a multi-channel spectrometer (Canberra InSpector 1000), connected to a PC equipped with spectra analysis software (Genie 2000). Count times of all samples were varied (3–10 min) to ensure propagated counting errors of < 5%. All measurements were corrected for background and radioactive decay. ^{134}Cs and ^{85}Sr emissions were counted at 605 and 514 keV respectively. Live crabs were radioanalysed using the method described by Cresswell et al. (2017b). This method, including animal rinsing, rinsing validation, errors associated with live-animal movement during radioanalysis and geometry corrections are detailed in the Supporting information.

2.4. Long-term exposure to dissolved species

A second dissolved radionuclide exposure was conducted using the same nominal exposure activity concentrations of ^{134}Cs and ^{85}Sr as above, but for 8–14 weeks to generate long-term uptake rate information for *P. laevis*. Ten crabs were exposed individually to each radionuclide in isolation (e.g. a total of 20 crabs were exposed for this experiment). Exposure solutions were renewed (100%) daily for the first 2 weeks then twice weekly and finally once weekly. Water samples were collected and radioanalysed pre- and post-water changes and radioanalysed to determine exposure activity concentration. Following exposure for 8 weeks, a subset of crabs was depurated in clean estuarine water with no addition of radiotracers, while others remained in exposure solution. Crabs were radioanalysed live during exposure and depuration as described above. During the exposure several crabs moulted (ecdysis), which affected the bioaccumulation rate of both ^{134}Cs and ^{85}Sr. Moulted crabs were monitored and treated as the non-moulted crabs to determine the significance of this physiological event. Although the exposure was conducted over 14 weeks, there was no substantial growth in individual crabs during this period. Intermoult crabs (n = 15) had a mean ± SD growth rate of − 0.001 ± 0.004 g/d. Moulted crabs were the only individuals to demonstrate a positive growth rate over 14 weeks: 0.012 ± 0.006 g/d (mean ± SD; n = 4).

2.5. Determining dietary assimilation of radionuclides using a pulse-chase method

P. laevis and other mangrove crabs are primarily detritivores with fine benthic organic matter constituting a significant proportion of their diet (verified by stable isotope mixing models) and are observed to feed off the surface layer of sediment (Mazumder and Saintilan, 2010). To determine the dietary assimilation efficiency (AE; the % of an element that is assimilated into internal tissues from the gut) of Cs and Sr by *P. laevis*, a synthetic food was formulated using commercial food pellets, spiked with ^{134}Cs and ^{85}Sr and gelled using agar as described in the Supporting information. Each spiked food pellet had a nominal activity of 1.7 and 2.2 kBq (52 and 67 kBq/g) of either ^{134}Cs or ^{85}Sr respectively (as pellets were produced separately for each isotope). The use of synthetic food to experimentally determine dietary AE is justified as Metian et al. (2019) concluded that the type of food ingested by marine organisms has little impact on the AE of Cs. No data are available on the impact of food type on the AE of Sr.

Active food pellets were fed to six individual crabs (16.3 and 20 mm carapace length and width respectively; 6.6 g ww) that had not been fed for three days before the experiment. Each crab was placed in an individual cylindrical 250 mL polystyrene vial with no water and fed one active food pellet by hand using a plastic spatula. Crabs ingested the food rapidly (< 5 min), every time food was provided and were immediately rinsed (Supporting information) and radioanalysed. Crabs were subsequently transferred to clean 1.125 L containers with clean estuarine water and fed non-active food pellets ad-libitum. Individuals were radioanalysed during this 'chase' period at intervals of 6 h, 1, 2 d and then every 1–2 days for a period of 23 d depuration.

2.6. Direct and indirect exposure to radiolabelled sediment

We hypothesised crabs would bioaccumulate the significant proportion of Cs and Sr from sediment i.e. both elements will preferentially sorb to fine sediment rather than exist in solution (partition coefficients > 100 L/kg; Carroll et al., 1999). As the study species predominantly feed on microphytobenthos on the surface layer of sediment (Mazumder and Saintilan, 2010), it stands to reason crabs would be exposed to Cs and Sr associated with sediment through their diet. To estimate the contribution sediment has compared to a soluble exposure for Cs and Sr bioaccumulation, crabs were exposed to sediment labelled with both ^{134}Cs and ^{85}Sr either directly or indirectly (i.e. caged above the sediment) as per a similar design to Cresswell et al. (2014b). Sediments were radiolabelled as described in the Supporting information.

30 mL of the homogenised labelled sediment was transferred to each of sixteen, 1.1 L exposure chambers and a further 970 mL of clean seawater was added to each container resulting in approximately 5 g (ww)/L of labelled sediment. The suspensions were left to settle for 24 h before polypropylene baskets were added to six of the containers (positioned 10 mm above the bottom of each container as the indirect treatment) and all containers received constant gentle aeration via an air hose for an equilibration period of 72 h before the introduction of crabs. Three containers were used as controls with no addition of crabs to determine the passive dissolution of both isotopes from the sediment to the overlying water.

Before the addition of an individual crab to each container (7 crabs for direct treatment, 6 crabs for the indirect treatment) a 10 mL sub-sample was collected from each container, filtered (< 0.45 μm) and radioanalysed. The exposure was conducted for 7 d with no renewal of water. Daily sub-samples of water were collected, filtered and radioanalysed. Crabs were removed from the containers daily, rinsed (Supporting Information) and radioanalysed. Crabs were fed outside the exposure containers during radioanalysis every second day. Following 7 d of exposure, crabs were depurated in clean, non-active estuarine water or 7 d to compare depuration kinetics between treatments and with the previous dissolved exposures.

2.7. Whole-body autoradiography and synchrotron X-ray fluorescence analysis of tissue sections

To determine the biodistribution of accumulated radionuclides within exposed crabs, two imaging techniques were used. Crabs from dissolved and dietary exposures (n = 3 for each) were randomly removed from experiments at pre-determined times and were rinsed (Supporting information), euthanized, embedded, flash-frozen and stored at − 80 °C until cryosectioning. Briefly, crabs were euthanized in a refrigerator at 4 °C for > 1 h. Body measurements of fresh weight, carapace length and width were recorded then the whole animal was embedded in Cryomatrix® (Thermo Scientific) within a petri dish and snap-frozen in liquid nitrogen. Sagittal sections (50 μm thick) were collected using a cryomicrotome (Cryostat Leica CM3050 S, Leica Biosystems) and were mounted on either poly-L-lysine coated glass slides or adhesive Kapton tape (Caplinq Europe, Netherlands). Where sections were mounted on Kapton tape, the tape was affixed to a glass slide using two thin strips of double-sided tape such that the adhesive of the Kapton faced away from the glass slide. Sections were immediately dehydrated using a freeze-dryer and stored in slide boxes once dry. Images of the blockface within the cryostat were collected, corresponding to each tissue section for anatomical orientation. Radioisotope localisation was assessed using photostimulated luminescence via phosphor plates

(autoradiography) of crab tissue sections, as per our previous studies (Cresswell et al., 2015, 2017a) and is described in the Supporting information. Autoradiography sections presented in the results and discussion section are collected from individual crabs. Each tissue section of interest was collected from at least three individual crabs and suggested that radionuclide localisation was reproducible among individuals (data not shown).

The X-ray fluorescence microprobe (XFM) beamline at the Australian Synchrotron was used to acquire high-resolution elemental maps of tissue sections. Freeze-dried Kapton tissue sections (from one individual crab) were fixed to a Perspex frame sample holder, which was mounted onto a high precision positioning stage. A 16 KeV incident energy beam was focused on 2–3 μm through a Kirkpatrick-Baez mirror system. The samples were scanned through this beam and the resulting fluorescence spectra were collected using the Maia 384 large solid-angle detector, applying the dynamic analysis method described by Ryan et al. (2010). The data was collected and analysed using GeoPIXE (http://www.nmp.csiro.au/GeoPIXE.html).

2.8. Radionuclide concentrations in crab organs following solution exposures

While individual radionuclide exposures were conducted in Section 2.2 to understand the bioaccumulation kinetics of each radionuclide from solution, this exposure sought to identify the organ distribution of radionuclides following combined exposure, as radioanalysis of organs of both radionuclides can be conducted simultaneously. A combined ^{134}Cs and ^{85}Sr exposure was conducted with six crabs (7.9 ± 1.4 g ww) to 47 ± 2.7 and 46 ± 4.9 kBq/L of ^{134}Cs and ^{85}Sr respectively for 14 d (exposure solution renewed every 2–3 days). The exposure was conducted as per Section 2.2 with crabs radioanalysed every 2–3 days. After 14 d exposure, crabs were rinsed (Supporting information), radioanalysed, euthanised and their mass and body measurements recorded. The uptake rates of the concentration factor (CF) over 14 days (calculated as the linear regression of CF over time; 0.24 and 0.34 g/mL/d for ^{134}Cs and ^{85}Sr respectively) were comparable to those determined in the previous solution exposure (Section 2.2). Organs were subsequently dissected and transferred to pre-weighed 10 mL polycarbonate vials, weighed (wet weight; ww) and dried at 60 °C for > 48 h. After cooling to room temperature in a desiccator, vials were re-weighed to obtain the dw of each organ. Organs were digested following a method described by King et al. (2004) as described in the Supporting information.

2.9. Biodynamic modelling of water and dietary contributions to crabs

To estimate the relative contribution of radionuclides from water vs. from diet, the steady-state, one-compartment global biodynamic model described by Landrum et al. (1992) was used. The model describes the steady-state radionuclide concentration (C_{ss}, Bq/g) as

$$C_{ss} = (k_u \times C_w)/(k_{ew} + g) + (AE \times IR \times C_f)/(k_{ef} + g) \quad (1)$$

Where k_u is the uptake rate constant of radionuclide from the aqueous phase (mL/g/d), C_w is the dissolved radionuclide concentration (Bq/mL), AE is the assimilation efficiency from food (%), IR is the daily ingestion rate of food by the organism (g/g/d), C_f is the radionuclide concentration in food items (Bq/g), k_{ew} and k_{ef} are the radionuclide efflux rate constants following ingestion and uptake from the aqueous phase respectively (d^{-1}), and g is the growth rate constant of the animal (d^{-1}). Published data from an accidental radionuclide release scenario (FDNPP) were used for C_w and C_f over differing time scales and values for IR were used from published studies that determined this factor for Asian shore crabs (Wang et al., 2016a). See Supporting Information Table 1 for reference data used in the biodynamic model.

As the main goal of the current study is to evaluate the relative contribution of water vs. diet to bioaccumulated concentrations of ^{134}Cs and ^{85}Sr during relatively short-term experiments, the growth of the animal was considered negligible and was not included. The parameters k_u, k_{ew}, k_{ef} and AE were evaluated from the experiments listed above using radiotracers, as has been demonstrated by numerous studies (Wang and Ke, 2002; Cresswell et al., 2014a; Wang et al., 2016a). Specifically, whole body uptake and depuration kinetics were fitted using nonlinear regression routines and iterative adjustment (Statistica® 7) and statistical methods described by Metian et al. (2016). A description of the derivation of biokinetic parameters and assumptions used in the biodynamic modelling procedure are provided in the Supporting information.

2.10. Statistical analyses

In order to determine changes to the uptake rate of each radionuclide over increasing exposure duration (e.g. 2–10 h, 2–25 h, 2–97 h, 2–169 h and 2–336 h), uptake models were assumed to be linear through the regression behaviour of radionuclide uptake rates (Fig. 1; Section 3.1). The quality of the regression was assessed through the Shapiro-Wilk test for measuring the normality of the regression residuals and Q-Q plots to compare the distribution of the standardised residuals to a normal distribution. A linear regression two-way ANOVA was performed to detect any differences between the uptake rates of each radionuclide over increasing exposure periods, followed by Tukey's post-hoc test for significant comparisons. Differences between the means of each time period were significant with a $p < 0.05$.

Differences in calculated biokinetic parameters (uptake and loss rate constants; CF_{ss}; Section 3.4) for the medium-term and long-term exposures of each radionuclide were determined using a one-way ANOVA. Prior to statistical analysis, tests for normal distribution of the data and Bartlett's homogeneity of variance test were conducted. No post-hoc tests were performed as there were only two groups within the factor variable (medium- & long-term exposure). Differences between the means of biokinetic parameters were significant within a $p < 0.05$.

Prior to statistical analysis of organ radionuclide concentrations (Section 3.6), tests for normal distribution of the data and homogeneity of variance test were conducted. Normal distribution was met so the data was not log transformed. Bartlett's test was performed and determined the variances in the concentration of each radionuclide was not the same across all the organs. A one-way ANOVA was used to detect any differences between organs, followed by Tukey's post-hoc test for comparisons. Differences between the means of organ concentrations were significant with a $p < 0.05$.

All statistical analyses of described above were conducted using R Studio V1.2.1 (R Core Team, 2020). All other statistical analyses of data were conducted with Student's T-tests after conducting F-tests to determine homogeneity of variance. These analyses were performed using Microsoft Excel.

3. Results and discussion

3.1. Dissolved exposure

Radioanalysis of exposure water subsamples revealed the time-average activity concentrations were relatively constant (49 ± 3 and 55 ± 3 Bq/mL for ^{134}Cs and ^{85}Sr respectively; Supporting information Fig. 3). Individual crab radioanalyses (in Bq/whole live animal) were converted to an activity concentration per mass of fresh tissue (e.g. Bq/g ww) plotted against exposure and depuration time (Fig. 1).

There was a good agreement among the 8 replicates for bioaccumulation of both radionuclides as demonstrated by the relatively minimal variance for both uptake and depuration curves. Following 14 days of continuous exposure, neither radionuclide reached equilibrium within the crabs, although ^{134}Cs demonstrated a greater tendency toward equilibrium over the exposure period (Fig. 1a). Uptake rate constants were determined using non-linear regressions of crab whole-body

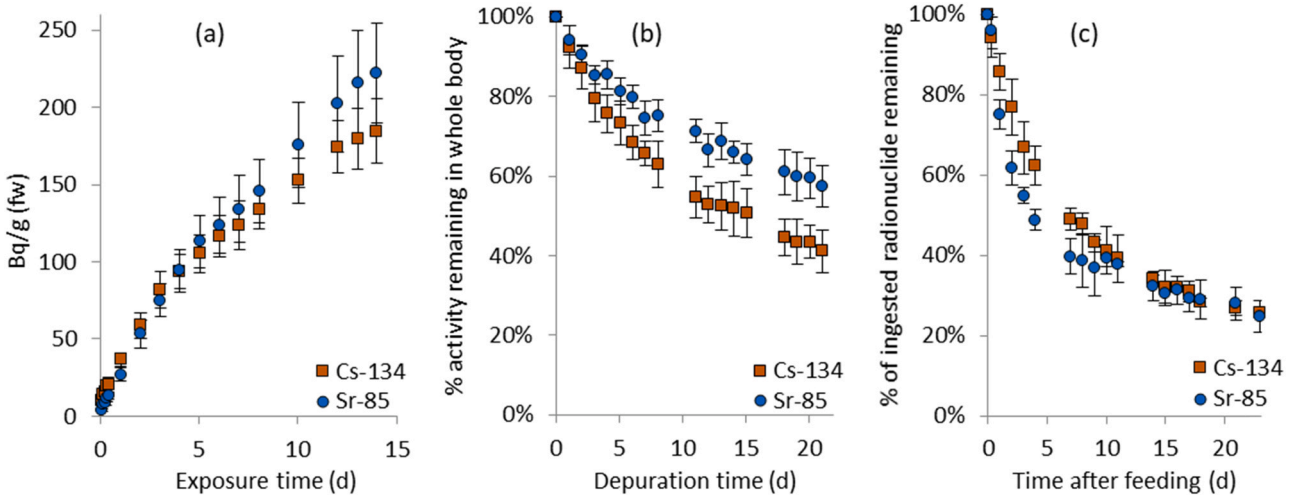

Fig. 1. Whole-body kinetics of ^{134}Cs and ^{85}Sr by adult male mottled shore crabs (*Paragrapsus laevis)* exposed to radionuclides (a) in solution during the uptake phase, (b) retention of radionuclides during depuration in radionuclide-free water following aqueous exposure, and (c) retention of radionuclides during depuration in radionuclide-free water following dietary exposure. Data collected from repeated live-measurements on the same individuals. No moulting occurred during uptake or depuration phases. Data shown are means ± 95% CI ($n = 8$ for (a) and $n = 6$ for (b) and (c)).

radionuclide concentrations over the 14 d of exposure as described in Section 2.9 and are provided in Table 2.

Many previous studies have derived uptake rate constants using linear regressions of whole-animal radionuclide concentrations over shorter periods of exposure (< 30 h) to determine uptake rate parameters in the absence of depuration processes (Wang and Ke, 2002; Wang and Wong, 2003; Lee and Lee, 2005; Dutton and Fisher, 2014). To investigate differences in exposure-period specific linear uptake rate constants, linear regressions of crab whole-body radionuclide concentrations over time were conducted. The uptake curves (Supporting information Fig. 4) for 0–10 h show a linear uptake rate between 2 and 10 h exposure but a substantially faster uptake rate from 0 to 2 h exposure. This resulted in derived linear uptake rates 3.8 and 1.8 times faster for ^{134}Cs and ^{85}Sr, respectively, for the initial 0–2 h of exposure compared with 2–10 h exposure. This suggests a fast-filling compartment immediately upon exposure, most likely the gill epithelial cells and adsorption to the cuticle, followed by the filling of an intermediate compartment from 2 to 10 h exposure that likely has some components of depuration. However, there were no significant differences ($p > 0.05$) in the uptake rates of either radionuclide for exposure periods of 2–10 h, 2–25 h, and 2–97 h (Table 1). This suggests biological regulation processes (i.e. combination of radionuclide uptake and depuration) were well established after two hours of exposure. This is contrary to other studies where exposures are conducted over a period of < 30 h to determine uptake rate parameters in the absence of depuration processes Our data suggest it is important to increase our understanding of exposure period on the uptake and elimination of radionuclides in decapod crustaceans, especially when deriving bioaccumulation parameters from relatively short exposure periods.

Depuration from live crabs in isotope-free water for both radionuclides (Fig. 1b) followed two-component exponential depuration models, with a greater proportion of ^{85}Sr being retained after 21 d (57 ± 5%) than for ^{134}Cs (41 ± 5%). Depuration rate constants were derived as per Section 2.9 and are provided in Table 2.

Table 1
Comparison of the uptake rates for different periods of exposure to ^{134}Cs and ^{85}Sr. Uptake rates (k_u) calculated as the linear regression of whole body radionuclide content for the exposure period specified. Data represent means ± S.D (n = 4). Different superscript letters ($^{a,\ b}$) represent a significant difference among k_u ($p < 0.05$; one-way ANOVA).

Radionuclide	Exposure period	k_u ($^{-1}$d)
^{134}Cs	2–10 h	1.3 ± 0.4^a
	2–25 h	1.1 ± 0.2^a
	2–97 h	0.9 ± 0.2^a
	2–169 h	0.7 ± 0.1^b
	2–336 h	0.5 ± 0.1^b
^{85}Sr	2–10 h	1.1 ± 0.2^a
	2–25 h	1.0 ± 0.4^a
	2–97 h	1.0 ± 0.2^a
	2–169 h	0.9 ± 0.2^b
	2–336 h	0.7 ± 0.1^b

3.2. Long-term dissolved exposure

Data on long-term (i.e. longer than 1–2 week laboratory studies) uptake in crustaceans is scarce. Extended exposures were conducted to provide more complete biokinetic uptake data including longer-term trends toward equilibrium (up to 14 weeks exposure) and prolonged

Table 2
Summary of biokinetic parameters ^{134}Cs and ^{85}Sr in mottled shore crab (*Paragrapsus laevis*) exposed these radionuclides through the dissolved (from medium- and long-term exposures) and dietary pathways. Values are means ± ASE (asymptotic standard error). For all values, probability of the model adjustment (p) are < 0.001 other than those with*.

	^{134}Cs	^{85}Sr
Aqueous exposure (n = 8)		
Uptake rate constant from aqueous phase (k_u, d^{-1})	0.63 ± 0.12^a, 0.41 ± 0.04^b	0.49 ± 0.11^a, 0.55 ± 0.26^b
Loss rate constant from aqueous phase (k_{ew}, d^{-1})	0.02 ± 0.03^{a,*}, 0.024 ± 0.004^b	0.02 ± 0.01^a, 0.004 ± 0.001^b
$T_{b1/2\text{-aqueous}}$ (d)	30 ± 33^{a,*}	35 ± 8^a
CF_{SS} (unitless)	4.4 ± 0.6^a, 8.6 ± 0.6^b	6.0 ± 0.7^a, 19 ± 2^b
Dietary exposure (n = 6)		
Assimilation efficiency (AE, %)	55 ± 10	49 ± 3
Ingestion rate (IR, g g^{-1} d^{-1})	0.14^c	0.14^c
Loss rate constant from dietary phase (k_{ef}, d^{-1})	0.04 ± 0.01	0.03 ± 0.00
$T_{b1/2\text{-dietary}}$ (d)	20 ± 6	24 ± 4

* p > 0.05.
[a] Model prediction from 14-day aqueous exposure and 21-day depuration (medium-term exposure).
[b] Model prediction from 56-day aqueous exposure and 51-day depuration (long-term exposure) using intermoult crabs only.
[c] For Japanese shore crab (*Hemigrapsus sanguineus*) feeding ad libitum on polychaete prey (Wang et al., 2016a).

depuration (up to 7 weeks). The time-averaged exposure activity concentration over 14 weeks was 50 ± 1 and 45 ± 1 Bq/mL for ^{134}Cs and ^{85}Sr respectively (mean ± 95% CI, $n = 68$; Supporting information Fig. 5). Long-term exposure biokinetic data was determined as per Section 2.9 and presented in Section 3.4.

After 8 weeks (56 days) of exposure, neither radionuclide reached equilibrium/steady state in crabs (Fig. 2). This is in stark contrast to Sezer et al. (2014), who found radiocaesium reached saturation in the marine shrimp *Palaemon adspersus* after 27 days exposure to 2.5 kBq/L nominal ^{134}Cs. It may be our exposure concentration used in this study (nominal 50 kBq/L) resulted in an increased time to equilibrium. Previous experimental studies of the euryhaline crab *Carcinus maenas*, exposed to 185 kBq/L ^{134}Cs determined steady-state equilibrium was reached in approximately 19 days (Bryan, 1961). As the *C. maenas* exposure was 3.7 times greater concentration, one would have expected that *C. maenas* reached equilibrium faster than *P.laevis* (greater exposure concentration = increased uptake rate). However, for *P.laevis* not to begin to approach equilibrium in 100 days (5.3 times longer than for *C. maenas*), this suggests substantial differences in radionuclide bioaccumulation and internal regulation processes between the two species. A study conducted by Schurr and Stamper (1962) exposed the freshwater crayfish *Cambarus longirostris* to 3.7 Bq/mL ^{85}Sr and suggested individuals reach 95% equilibrium after 4–10 days. This is substantially more quickly than *P. laevis* in our study, which did not reach equilibrium after 56 days. This may be due to the euryhaline nature of estuarine decapods compared to solely freshwater organisms. *P. adspersus* reached a whole body steady state CF (CF_{ss}) of approximately 15 (Sezer et al., 2014), while after 14 weeks of exposure in our study, intermoult *P. laevis* reached a CF_{ss} of approximately 11 and had yet to reach equilibrium. It is clear that there are multiple factors governing the time for decapod crustaceans to reach steady state and the extent of such equilibrium with radionuclides in solution.

3.3. Effects of moulting on radionuclide bioaccumulation

During the exposure and depuration phases, several crabs moulted. This common and frequent physiological change in crustaceans had substantial effects on the bioaccumulation of both ^{134}Cs and ^{85}Sr (Fig. 2). One crab moulted at day 30 during exposure to ^{134}Cs and demonstrated an increased uptake rate relative to the general population of intermoult (non-moulted) crabs for 13 days before moulting (Fig. 2a). The individual also did not eat food offered to it 7 days before moulting. The crab's whole body ^{134}Cs burden remained stable for 3 days post-moult, then reduced its whole-body ^{134}Cs burden for 11 days before returning to the same uptake rate as for intermoult crabs. During this 11 day period, the individual crab lost 13% of its whole body ^{134}Cs. While there was only a single specimen in the ^{134}Cs experiment that moulted during depuration, the data suggests post-moult physiological processes were responsible for the depuration of ^{134}Cs under constant exposure to aqueous ^{134}Cs, especially compared to all other intermoult crabs, which continued to accumulate ^{134}Cs. Sezer et al. (2014) recoded a similar phenomenon during solution exposure of the shrimp *P. adspersus*, where 15.3 ± 8.1% of total body burden was eliminated with moulting.

A possible explanation for this post-moult loss of ^{134}Cs maybe that pre-moult, the crab increases its accumulation of water to swell its body to 'crack' its shell during moulting. As the internal water content of the crab increases, potassium uptake from the surrounding media also increases. As Cs is a potential surrogate for K active transport in vivo, ^{134}Cs uptake rate may also increase (as shown in our data; Fig. 2a). The 'extra' ^{134}Cs likely accumulated in a very labile form not associated with internal tissues to any significant degree. After moulting, the crab releases the extra water back to the surrounding media and hence a potential loss of K and ^{134}Cs. During this process, the crab lost approximately 17% of its total body burden of ^{134}Cs.

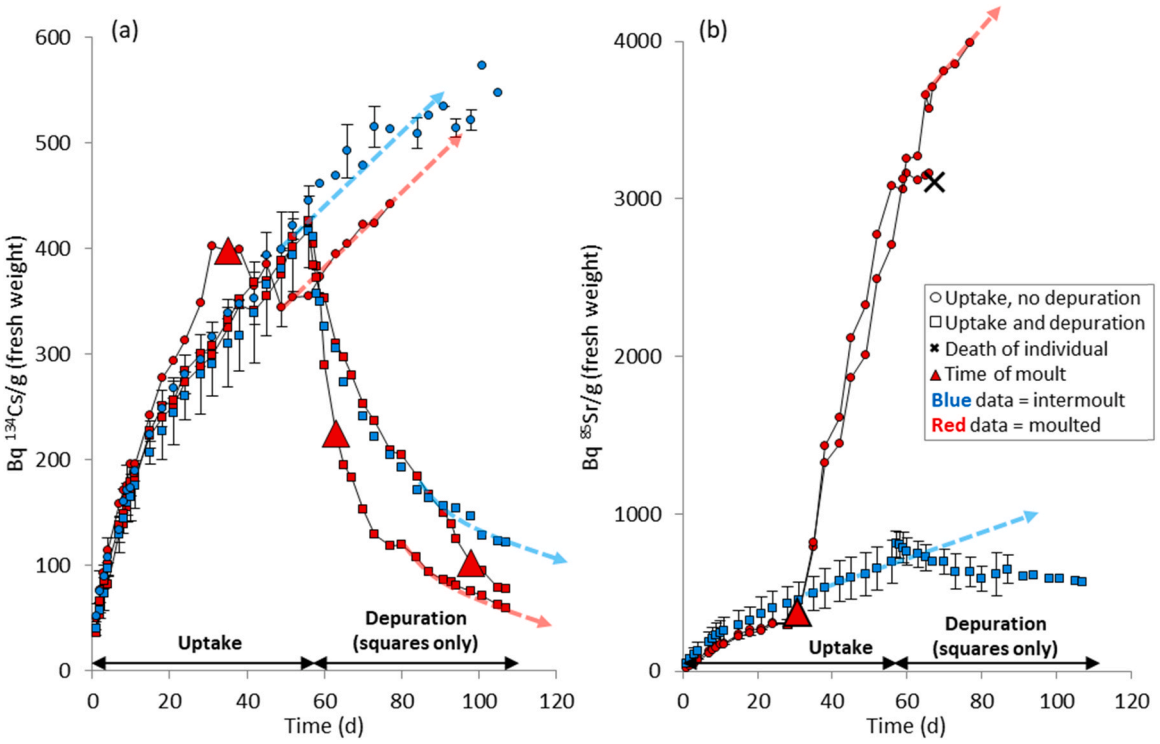

Fig. 2. Long-term uptake and depuration profiles of ^{134}Cs (a) and ^{85}Sr (b) by adult mottled shore crabs (*Paragrapsus laevis*) exposed to 50 ± 1 and 45 ± 1 Bq/mL respectively. Blue data points represent the mean ± 95% CI (n = 1–6) activity concentration of intermoult (non-moulted) crabs while red points represent individual crabs that moulted. The generalised linear uptake and depuration profiles of ^{134}Cs and uptake profiles of ^{85}Sr by post-moult crabs are represented by dashed red arrows while those of intermoult crabs are represented by dashed blue arrows (For interpretation of the references to colour in this figure legend, the reader is referred to the web version of this article).

In the same ^{134}Cs experiment, two other crabs moulted during the depuration phase and again demonstrated an increased depuration rate relative to the single intermoult crab also undergoing depuration (Fig. 2a). The first crab that moulted during depuration displayed an increased depuration rate for 20 d before returning to a similar depuration rate as the intermoult crab (depicted on Fig. 2a by red and green dashed arrows respectively). These data indicate that moulting substantially affects the bioaccumulation of ^{134}Cs in *P. laevis*. Moulting was also shown to affect the loss of ^{134}Cs in the marine decapod *Penaeus stylirostris* during depuration in clean water, where ^{134}Cs was determined in the released exuviae, especially following dietary exposures (Metian et al., 2016).

The bioaccumulation of ^{85}Sr was also considerably affected by moulting with two individual crabs moulting on day 28 of exposure (Fig. 2b). Both crabs demonstrated a substantial increase in ^{85}Sr uptake rate post-moult, with both individuals displaying very similar uptake rates to each other. These moulted crabs continued to accumulate ^{85}Sr at a greater uptake rate than intermoult crabs and during the final 10 d of exposure (days 67–77 of exposure) before the experiment was terminated, one moulted crab had an uptake rate of ^{85}Sr of 26.5 Bq/g/d compared with the intermoult crab's uptake rate of 9.5 Bq/g/d. The data suggests that 49 d post-moult, the moulted crab was still accumulating ^{85}Sr at a rate 2.8 times greater than that of the intermoult crab. By exposure day 60 (32 d post-moult), one of the moulted crabs reduced its accumulation of ^{85}Sr to near-zero uptake rate and ate very little of the food provided to it for the following 7 d. On day 67 of exposure, that crab was found to be dead in its tank, suggesting a grave reduction in physiological processes which ceased the bioaccumulation of ^{85}Sr.

Moulting by decapod crustaceans has been seen to influence the bioaccumulation of other elements. For example, when the freshwater prawn *Macrobrachium australiense* moulted, ^{109}Cd uptake rate increased significantly relative to intermoult prawns 2 d post-moult (Cresswell et al., 2015). In the same study, ^{65}Zn was found to decrease immediately after moulting followed by an increase in uptake rate for several days post-moult. Mohapatra et al. (2009) found Ca, Cu, K and Mn were reabsorbed from the carapace to the body tissue in newly moulted mud crab *Scylla serrata*, presumably to meet ongoing metabolic requirements in the crabs and support the formation of the new carapace. The same study showed Pb was excreted to the cast-off shell during moulting, demonstrating a pathway to remove the element from body tissues. Our data show a potentially very large step increase in ^{85}Sr uptake by crabs due to moulting. It implies the results of laboratory studies that do not account for moulting may poorly represent real-world conditions where moulting is common. For crabs in natural conditions, it has yet to be determined how long it would take for the uptake rate of ^{85}Sr of post-moult crabs to reach the uptake rate of intermoult crabs. Furthermore, it is currently unknown how long the moult cycle is for *P. laevis* and we are therefore unable to estimate what proportion of the moult cycle is affected by this increase in ^{85}Sr uptake. Further research into the effects of moulting on Cs and Sr regulation by estuarine crabs is necessary to increase our understanding of the impact of this physiological process on common radionuclide bioaccumulation patterns, especially when attempting to interpret field whole-body burden data with only soluble radionuclide concentrations.

3.4. Dietary assimilation of radionuclides

Water samples taken during the first hours and days of the 'chase' period returned no activity above background levels, demonstrating there had been no or negligible cycling of soluble radionuclides during the 'chase' period (e.g. from the dissolution of radionuclides from faeces). The depuration profiles after dietary exposure differed from those from the aqueous exposures (Fig. 1). After 21 days of dietary depuration, approximately 28% of both radionuclides remained in the crabs (Fig. 1c), while after the same period of depuration following aqueous exposure, approximately 41% and 57% of ^{134}Cs and ^{85}Sr respectively remained in the crabs (Fig. 1b). This is not unusual owing to the different exposure periods and different biochemical uptake process occurring at the gill apical cell membranes compared to those of the gastro-intestinal system. However, the calculated medium-term loss rate constants for both radionuclides (Table 2) were not significantly different ($p > 0.05$, unpaired Student's *t*-test) for the aqueous depuration ($k_{ew} = 0.02 \pm 0.03$ and 0.02 ± 0.01 d^{-1} for ^{134}Cs and ^{85}Sr respectively) compared to the dietary depuration ($k_{ew} = 0.04 \pm 0.01$ and 0.03 ± 0.00 d^{-1} for ^{134}Cs and ^{85}Sr respectively). This suggests that once assimilated into main internal tissues, the depuration processes for both radionuclides are similar, irrespective of exposure pathway.

Dietary depuration of cationic elements in decapods often follows a bi-phasic loss pattern (Cresswell et al., 2014a) with the fast loss phase (e.g. 0–24 h) representing the egestion of active dietary items within the gut retention time (GRT). This phase is followed by a slower loss phase considered to be the loss rate from internal tissues post gastric assimilation. AEs are calculated as the y-intercept of the non-linear regression of the slow loss phase. AEs calculated using the statistical modelling software (Section 2.9) were estimated as $55 \pm 10\%$ and $49 \pm 3\%$ for ^{134}Cs and ^{85}Sr respectively (Table 2). The AE for ^{134}Cs is very similar to the maximum ^{137}Cs AE reported for the Asian shore crab *Hemigrapsus sanguineus* of 55% when ingesting contaminated polychaete worms (Wang et al., 2016a). AE data for estuarine/marine crustaceans for Sr is scarce in the literature so we were unable to compare our data with previous reports of this parameter for comparable organisms.

3.5. Biokinetic parameters of radionuclide uptake and loss

Biokinetic parameters determined from the dissolved and dietary experiments were calculated using methods described in Section 2.9 for both uptake and depuration kinetics. Table 2 summarises the biokinetic parameters for both the medium-term (14-day aqueous exposure and 21-day depuration) and long-term (56-day aqueous exposure and 51-day depuration) aqueous exposures and dietary exposure. Loss rate constants were taken as the long-lived exponential component from the Statistica® 7 model output (e.g. k_{el}). Full uptake and depuration kinetic parameters are available in Supporting information Table 2 and 3 respectively.

CF_{SS} is the concentration factor; the ratio between whole-body activity (Bq g^{-1} ww) and time-integrated activity of radiotracers in seawater (Bq g^{-1}) at steady state.

Although the medium-term and long-term exposures were undertaken with the same species of crab, under the same laboratory conditions and to the same solution concentration of radionuclides, there were differences in the biokinetic parameters predicted by our modelling. For example, the calculated medium-term exposure k_u was 0.63 ± 0.12 d^{-1}, while that for the long-term exposure was 0.41 ± 0.04 d^{-1} for ^{134}Cs. However, there was no significant difference in the k_u values calculated for the first 10 days of exposure for both exposure periods (mean k_u values were 0.74 ± 0.18 and 0.71 ± 0.14 for medium- and long-term exposures up to 10 d respectively; $p = 0.73$; Student's T-test; equal variances). This suggests the uptake rate constants calculated for entire exposure periods only differ following prolonged (e.g. > 10 day) exposure. While there was no difference in the calculated loss rate constants for ^{134}Cs for the medium- and long-term exposures, the predicted CF_{ss} was significantly different ($p < 0.01$) at 4.4 ± 0.6 and 8.6 ± 0.6 respectively (Table 2). The differences in the calculated uptake rates from the two exposure periods were therefore responsible for the predicted CF_{ss}. Contrary to ^{134}Cs, the estimated uptake rate constants for the medium- and long-term exposures for ^{85}Sr were not significantly different ($p > 0.05$; Table 2). However, the calculated loss rate constants were significantly different ($p < 0.01$) by more than an order of magnitude, with the long-term exposure having a lower loss-rate constant (Table 2). This difference in calculated loss rate constants resulted in a significant difference ($p < 0.01$) in CF_{ss} between the medium- and long-term exposures at 6.0 ± 0.7 and 19 ± 2

respectively. Our data highlights the importance of selecting an exposure period that is appropriate for the aims/hypothesis being tested in each study when deriving biokinetic parameters.

Radionuclide concentration ratios (CRs) are used to describe the ratio of steady-state equilibrium within an organism as a result of absorption from both the seawater and from the food web, often using data from water and biota samples collected in the field (Howard et al., 2013). The wildlife transfer database (WTDB; IAEA & IUR) list the geometric means of CRs for adult marine crabs as 14 for Cs (n = 66) and 2.4 for Sr (n = 4) and. Table 2 shows the predicted concentration factor at steady state (CF_{ss}), which is the ratio between the activity concentration in the animal and the exposure concentration and does not account for contribution from dietary sources. Our data show the predicted CF_{ss} for Cs following the medium-term exposure was 4.2, which is 3.3-times less than the WTDB geometric mean of 14 (within reasonable agreement given the wide range of CRs reported in the WTDB; https://bit.ly/31ga9y7). These CRs for crab are low relative to other CRs in the database and suggests water sources of Cs are likely to be less significant than dietary sources for *P. laevis*, which is in agreement with other studies of marine benthic species (Johansen et al., 2015; Wang et al., 2016a). The predicted CF for ^{85}Sr was 6.0 for *P. laevis*, which is 2.5-times greater than the WTDB CR of 2.4 (also within reasonable agreement given the wide range of CRs reported). This suggests that compared with Cs, the water exposure pathway of Sr is more significant to *P. laevis*. Furthermore, differences between our CF and the WTDB CR for Sr seawater and biota samples from the Irish Sea and determined the mean CR of a range of marine crustaceans to be 56 (range of 13–99) for Sr. This value is substantially greater than that determined in our study. Further work is required to understand the factors affecting the bioaccumulation of Sr by marine crustaceans.

3.6. Accumulation of radionuclides from sediment

Daily filtered water radioanalysis (Supporting information Fig. 6) demonstrated there was no substantial difference in average dissolved concentrations of either ^{134}Cs or ^{85}Sr among treatments over the 7 day exposure period suggesting that the presence of a crab within an exposure chamber did not result in increased radionuclide dissolution from labelled sediments as has been shown for decapods exposed to sediments containing copper (Cresswell et al., 2014b). Furthermore, concentrations of dissolved ^{134}Cs and ^{85}Sr remained relatively constant over the 7-day exposure (Supporting information Fig. 7) suggesting that equilibrium between labelled sediments and the overlying solution was reached before the introduction of crabs. The whole-body bioaccumulation of ^{134}Cs and ^{85}Sr by crabs exposed to labelled sediments is shown in Fig. 3.

There were no significant differences in the whole-body accumulation profiles of ^{134}Cs by crabs exposed directly to sediment or caged above the labelled sediment receiving exposure to dissolved radionuclides (Fig. 4a; $p > 0.05$; unpaired Student's *t*-test). Since there was no difference in dissolved radionuclide concentrations between treatments (Supporting information Fig. 7), the data suggests bioaccumulation from dissolved ^{134}Cs (i.e. via uptake across the gills during respiration) was the significant uptake pathway. Furthermore, there was no discernable difference between the whole-body ^{134}Cs CF uptake profiles of crabs exposed to labelled sediment and those from the dissolved exposure described in Section 3.1 (Fig. 3c).

Only moulted crabs demonstrated sufficient whole-body ^{85}Sr concentrations for detection. During rinsing of the labelled sediment before the crab exposure, substantial ^{85}Sr was removed from the sediment (approximately 65%; Supporting information) suggesting the Sr was very loosely-sorbed to the sediment. Therefore the concentration remaining associated the sediment was greatly reduced. Indeed, mean solution exposure concentration was 3–4 kBq/L ^{85}Sr (Supporting information Fig. 7).

One crab from each of the direct and indirect treatments moulted (Fig. 4) on exposure days four and six. As had been found with the previous moulting during exposure to dissolved ^{134}Cs (i.e. Fig. 2), both crabs in the sediment exposure increased their whole-body uptake rate of the radionuclide before moulting. Similar to the solution-only experiment, the crab that moulted on day four of direct sediment exposure also had a net loss of ^{134}Cs uptake in the days following moulting, but ^{134}Cs was greatly decreased in this instance. Both moulted crabs then demonstrated increased depuration rates when transferred to clean water relative to the depuration rates of inter-moult crabs (Fig. 2). ^{134}Cs depuration profiles for crabs following sediment exposure (both direct and indirect) were similar to, if not slightly quicker than that from the dissolved radionuclide exposure (Supporting information Fig. 7). However, the differences in whole-body ^{134}Cs concentrations for the

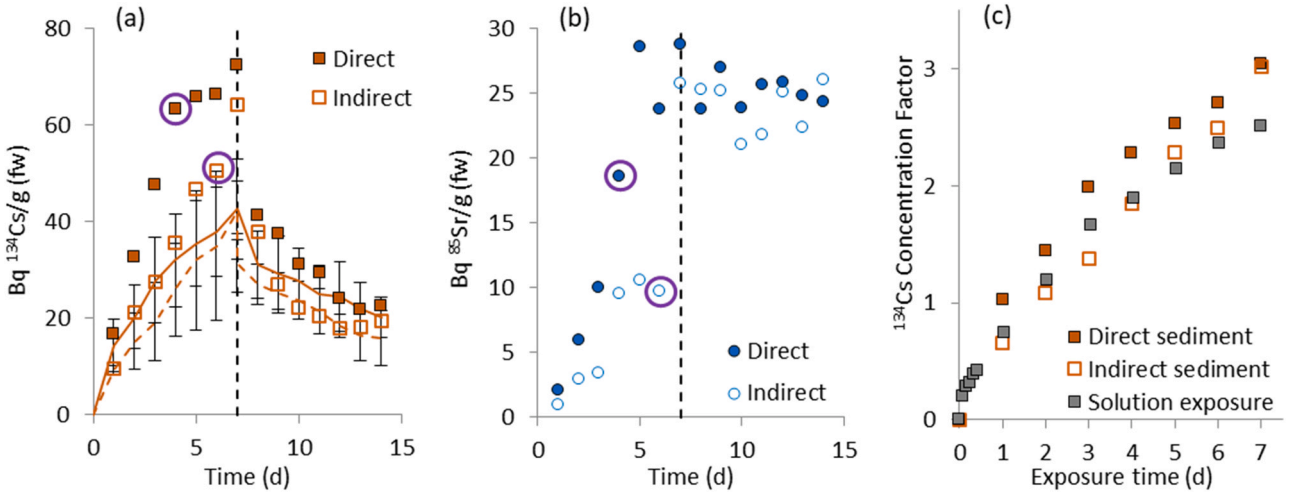

Fig. 3. Whole-body bioaccumulation of ^{134}Cs (a) and ^{85}Sr (b) by adult mottled shore crabs (*Paragrapsus laevis*) exposed to sediments labelled with both radionuclides, either directly or indirectly (i.e. caged above sediment). Data shown by lines (solid line = direct exposure; dashed line = indirect exposure) for ^{134}Cs are means ± 95% CI ($n = 5$). Individual crabs that moulted in both direct and indirect treatments are shown by individual data points for ^{134}Cs (a) and ^{85}Sr (b) and the time of moult is indicated by purple circles around data points. The period of transfer of crabs from exposure into clean water (depuration) is denoted by vertical dashed black lines in (a) and (b). ^{85}Sr in intermoult crabs were below detection limits and are not shown. Increases in crab whole-body concentration factor (CF) over the 7 day exposure to sediment are shown for ^{134}Cs (c) (means; $n = 5$) and are compared to increases in CF from the dissolved radionuclide exposure ("Solution exposure" data; grey squares; means; $n = 8$) (For interpretation of the references to colour in this figure legend, the reader is referred to the web version of this article).

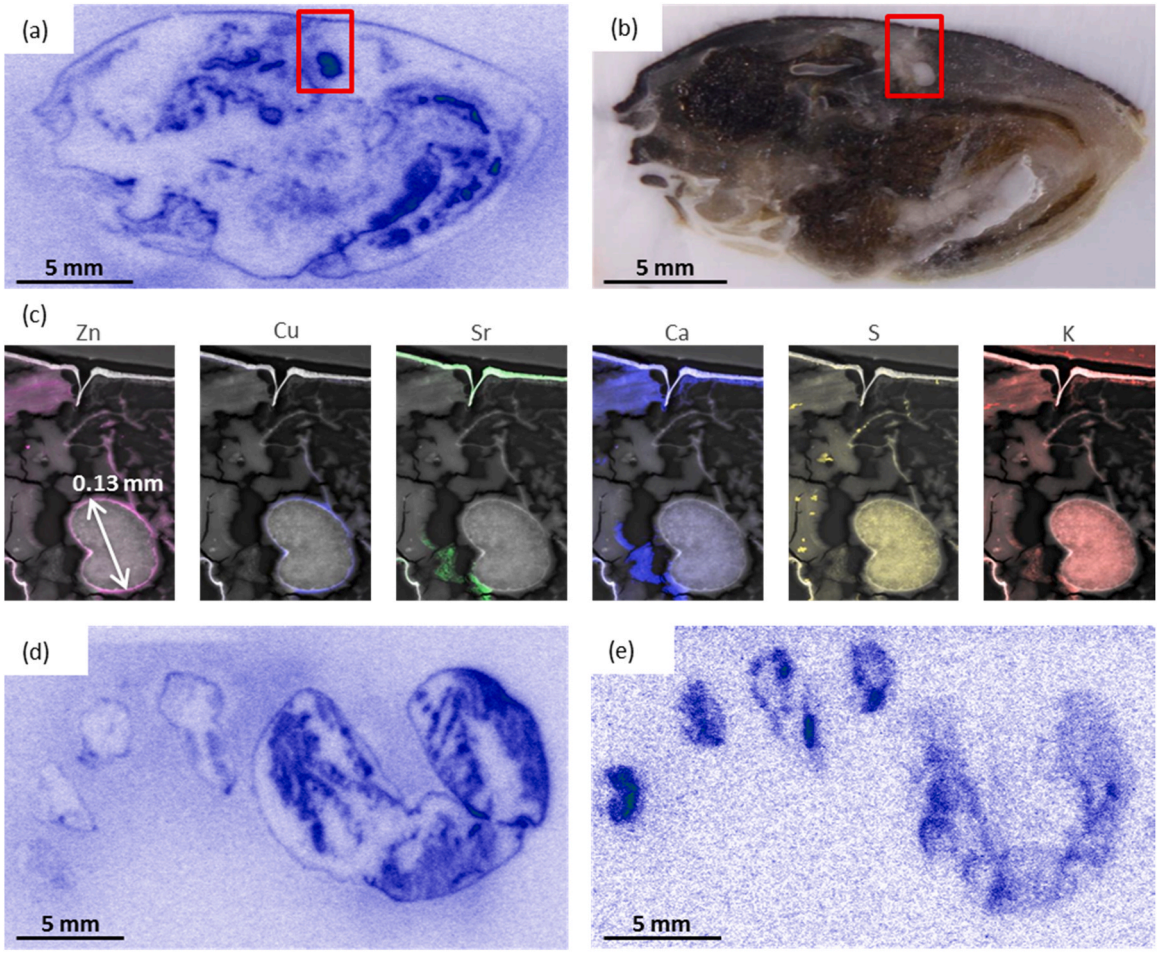

Fig. 4. False-colour images of ^{134}Cs and elemental distribution in tissue sections of an individual adult male mottled shore crab (*Paragrapsus laevis*) exposed to ^{134}Cs in solution for 14 weeks; (a) autoradiograph of ^{134}Cs biodistribution in sagittal section (crab facing left) with (b) corresponding colour photograph of block-face. The location of the gonad is highlighted with a red square in (a) and (b). XFM elemental maps of crab gonad (c) with the organ in the lower right of images and shell in top of maps. Distribution of ^{134}Cs in a sagittal section of the claw (large "U" shaped organ) and through pereiopods for same individual crab (d) are compared with tissue sections from an individual crab 6 h after ingestion of ^{134}Cs-labelled food (e). All tissue sections were 50 μm thick (For interpretation of the references to colour in this figure legend, the reader is referred to the web version of this article).

direct and indirect treatment crabs were not significantly different from those in the dissolved exposure after seven days of depuration ($p > 0.05$; Student's *t*-test).

As was seen previously with the long-term dissolved exposure, crabs that moulted during the direct and indirect sediment exposures (days four and six of exposure respectively) greatly increased their rate of whole-body ^{85}Sr uptake following moulting (Fig. 3). When the moulted crabs were transferred to clean water to depurate, both crabs retained their accumulated ^{85}Sr with no reduction in whole-body ^{85}Sr concentration following 7 days of depuration. This was in contrast to the intermoult crabs that did reduce whole-body ^{85}Sr during depuration (Fig. 1). The process of moulting led to the retention of accumulated ^{85}Sr during exposure to clean water conditions, presumably to assist with the formation of a new shell. Further studies on the impacts of moulting on Sr regulation should be undertaken, preferably with multiple decapod crustaceans all synchronised to moult simultaneously.

These results highlight the labelled sediments were acting as a source of dissolved radionuclides which were the predominant source of ^{134}Cs and ^{85}Sr to crabs. In the field, it is more likely both radionuclides will adsorb to fine sediments more strongly than was the case in this study where equilibrium during radiolabeling of the sediments was reached in a small volume of laboratory-conditioned sediments with representative organic matter in a closed system within a matter of days. Future studies should attempt to a larger volume of labelled solution, with a recirculating setup, and control for organic-physico structure to provide a more field-realistic sediment exposure.

3.7. Biodistribution of ^{134}Cs and ^{85}Sr following solution and dietary exposure

Sagittal sections of whole-crabs exposed to ^{134}Cs from solution suggested a broad distribution of ^{134}Cs across multiple internal organs (Fig. 4a), likely due to caesium being a surrogate for potassium (K) active transport in vivo (Bryan, 1961). Of all the organs able to be identified from the autoradiograph and corresponding block-face optical image with ^{134}Cs accumulation, there was a clear accumulation of the radionuclide in the gonad (red boxes in Fig. 4a and b). If the gonad is a significant site of Cs internalisation, this could potentially have implications for the reproductive success of crabs as ^{137}Cs (30 y half-life) has significant beta emissions at 512 keV (95% incidence) and at 1173 keV (5% incidence) that would provide a direct dose to the gonad. These tissue sections were examined with XFM elemental mapping and there were strong signals for sulphur (S) and K in the gonad (Fig. 4c), suggesting significant metabolic turnover that would be present in a gonad (the XFM method did not detect Cs due to k-edge interferences with silver (Ag)). Elemental mapping also showed zinc (Zn) and copper (Cu) surrounding the organ, likely demonstrating haemolymph circulation around the organ (Fig. 4c). Maps of strontium (Sr) and calcium (Ca)

show accumulation in the shell (at the top of the image), and some near the gonad (within 10 mm; Fig. 4c).

To determine whether there was a greater accumulation of ^{134}Cs in the gonad relative to other organs, six crabs were exposed to nominal concentrations of 50 kBq/L of ^{85}Sr and ^{134}Cs combined in solution for 14 d, individuals were euthanized, then their radionuclide organ burden was determined via organ dissection and gamma spectrometry. No individuals moulted during the exposure period. Of all the organs analysed, muscle tissue had the greatest mean ^{134}Cs concentration (Bq/g ww) and there was not more in the gonad than other organs (Fig. 5). There were no significant differences in ^{134}Cs concentrations among organs ($p > 0.05$).

The presence of radiocaesium in muscle tissue is well documented for vertebrates and invertebrates (Pinder et al., 2011; Harmelin-Vivien et al., 2012; Rowan, 2013a; Sohtome et al., 2014; Jeffree et al., 2015) and readily enters both human and non-human consumers via dietary transfer (Aarkrog et al., 1997). However, on average, ^{134}Cs is relatively well-distributed through all soft tissues, including those of crab (Caffrey and Higley, 2013), and therefore using a homogeneous whole-body approach to caesium internal distribution is often used when undertaking biota dose assessments using software such as the ERICA tool (Ulanovsky et al., 2008; Ruedig et al., 2015; Brown et al., 2016). Our results support this approach for *P. laevis* when assessing ^{134,137}Cs. However, ^{85}Sr was present in the gonad twice as much as compared to the next most concentrated organ; the brain (1004 ± 245 vs. 529 ± 91 Bq/g ww respectively; mean ± SE; $n = 6$). The gonad had significantly greater ^{85}Sr concentrations compared to all other organs ($p < 0.01$). This may have considerable implications for reproductive success as ^{90}Sr (the 30 year half-life isotope) has substantial beta emissions at 546 and 2284 keV (both at 100% incidence). Interestingly, the XFM elemental map of the gonad showed most strontium concentrated in a specific area within the gonad (Fig. 4c). The data suggest radiostrontium also concentrates at this location, which implies greater dose rates for those specific tissues. We believe this is the first report of radiostrontium significantly accumulating in dose-sensitive crab reproductive organs. Further research and bio-dosimetric modelling should be conducted to investigate the potential for population-level effects.

Autoradiographic imaging of sagittal sections of claws and pereiopods (Fig. 4d and e) revealed that there was substantial ^{134}Cs accumulation in the muscle tissue of these organs, confirming the findings of the organ dissection, digestion and radioanalysis. The autoradiographic images suggested ^{134}Cs was not homogeneously distributed across claw muscle tissue, but instead accumulated with what appear to be different muscle types of differing ^{134}Cs activity concentrations (Fig. 4d). Further work should be conducted in this area to better understand radio caesium accumulation in differing crustacean muscle fibres. While there was not as much ^{134}Cs within the claw and pereiopods 6 h after ingestion of labelled food (Fig. 4e) compared to 15 weeks exposure to ^{134}Cs in solution (Fig. 4d), there was a large enough signal-to-noise ratio to demonstrate the presence of ^{134}Cs in the claw. This suggests the bioaccumulation of radiocaesium across the gut, transfer via the haemolymph to the heart then subsequent transfer out to the extremity muscles occurs rapidly (i.e. < 6 h). Bryan (1961) determined the muscle tissue of the euryhaline crab *Carcinus maenas* was the slowest to accumulate ^{137}Cs, with other organs/body fluids accumulating more rapidly in the order of blood > urine > gills > excretory organ > hepatopancreas = muscle.

We believe this is the first reporting of internal biodistribution kinetics of ^{134}Cs from the diet in crabs and demonstrates a very short exposure duration (i.e. 5 min of feeding on Cs-contaminated food), will likely result in rapid transfer to organs that are likely to have slower depuration kinetics (i.e. muscle tissue), compared to gastro-intestinal organs would have a faster depuration rate (Rowan, 2013b).

Whole-body ^{85}Sr autoradiography did not yield any significant images, most likely due to the isotope having a very low incidence (< 1%) beta emission at 499 keV. The same tissue sections were interrogated by XFM to determine whether the Sr was purely adsorbed on to the external surfaces of the cuticle or whether Sr was homogenous across the depth of the shell. Elemental profiles of a cross-section of the crab's shell revealed Sr was indeed homogenously-distributed from the inside to the outside of the shell and mirrored calcium (Ca) distribution in the shell (Fig. 6).

While the XFM data only provides information on total Sr (i.e. all isotopes), bioaccumulated ^{85}Sr likely shared the same distribution pattern. Therefore supporting the hypothesis that an increase of ^{85}Sr bioaccumulation post-moult (as shown in the dissolved exposure) was likely due to the requirement of Sr in the new cuticle. XFM analysis also showed a thin layer of copper (Cu) on the inside of the cuticle, which likely represents the haemolymph and iron (Fe) on the outside of the cuticle, likely from adsorption of soluble Fe from the estuarine solution.

3.8. *Biodynamic modelling of water and dietary contributions of radionuclides to a marine crab using real-world data*

Biokinetic parameters for the medium-term aqueous exposure and dietary exposure (Table 2) were combined with ^{137}Cs and ^{90}Sr activity concentrations measured in seawater and benthic dietary items (e.g. fish, shellfish, seaweed, benthic invertebrates) collected near the FDNPP accident site. Three simplified conditions were modelled using monitoring data from 0.5 to 10 km distance from the FDNPP: pre-accident activity concentrations sourced from general Japan coastal data; the first three months following the accident; and 1–3 years following the accident (Supporting information Table 1). The model was not intended

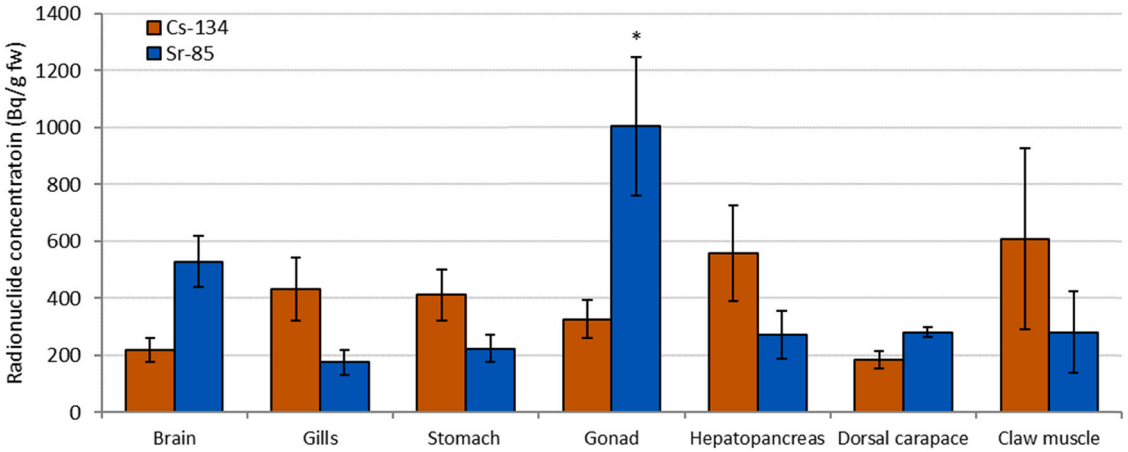

Fig. 5. Tissue distributions of ^{85}Sr and ^{134}Cs in adult mottled crabs (*Paragrapsus laevis*) following 14 d exposure to 50 kBq/L and no moulting. Data shown are mean ± SE ($n = 6$). * ^{85}Sr in gonad is significantly higher than all other organs ($p < 0.01$).

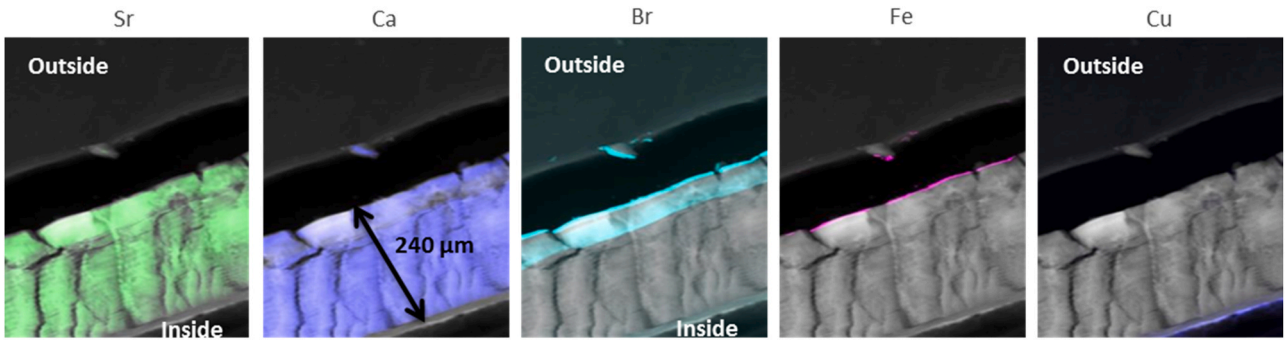

Fig. 6. False-colour synchrotron X-ray fluorescence microscopy (XFM) maps of elemental distribution through a cross-section of post-moult individual adult mottled shore crab (*Paragrapsus laevis*) shell following exposure to ^{85}Sr in solution (50 kBq/L nominal exposure) for 12 weeks.

to be highly calibrated to FDNPP conditions, rather, is intended to test dietary vs. water-sourced uptake of radionuclides at activity concentrations ranges that may occur during large-scale coastal accidental releases. Several key assumptions were made for the biokinetic model as described in the Supporting information.

The biokinetic model (Fig. 7) suggests pre-accident, diet would have been the significant source (97%) of ^{137}Cs to crabs. However, shortly after the FDNPP accident, water was the dominant source (99%) due to an increase in dissolved ^{137}Cs activity concentrations by up to 6 orders of magnitude. In the 1–3 years following the accident, the model predicted diet would return as the main source of ^{137}Cs to crabs (89%). These results are consistent with observed conditions where several months after the accident, the ^{137}Cs concentrations in seawater greatly reduced while levels in sediments and general marine organisms (e.g. crab diet sources) remained elevated and decreased much slower (Johansen et al., 2015; Wada et al., 2016). Our simplified model predictions are in general agreement with other laboratory studies such as Wang et al. (2016a), who determined the Asian shore crab (*Hemigrapsus sanguineus*) accumulates only 1.2–2.5% of whole-body Cs from the aqueous phase when not exposed to significant dissolved activities. Mathews and Fisher (2009) demonstrated Cs can be appreciably accumulated from the dissolved phase by marine elasmobranch and teleost fish depending on the prey selection. Our model outputs are also in agreement with field studies conducted in the waters off the east coast of Japan in the years following the FDNPP accident, suggesting the dietary pathway and specifically a sediment-associated diet is largely responsible for the prolonged ^{137}Cs bioaccumulation (Bezhenar et al., 2016; Wang et al., 2016b). From a perspective of dose, the model predictions highlight that, under scenarios of significantly increased Cs release to water (either directly or via atmospheric deposition), the predominant source of ^{137}Cs to crustaceans can shift from diet to water and substantially-elevated dose rates may occur during this period.

The biodynamic model predictions for ^{90}Sr accumulation also suggest increased contribution from the water pathway after a large scale release (Fig. 7b). The model predicted that under pre-accident conditions, 59% of bioaccumulated ^{90}Sr would be from the water with 41% from dietary items. These predictions suggest the water pathway is most important in a wide range of release conditions for ^{90}Sr bioaccumulation in *P. laevis*. Indeed, when the model was computed with the comparable ^{90}Sr activity concentrations determined soon after the accident (3.6 Bq/L for water and 4 Bq/kg ww for dietary sources; Supporting information Table 1), the water exposure pathway was predicted to account for 91% of whole-body ^{90}Sr in *P. laevis*, while dietary sources accounted for only 9% (Fig. 7b). In the 1–3 years following the FDNPP accident, dissolved ^{90}Sr activity concentrations decreased to approximately 0.8 Bq/L, while dietary items were approximately 2 Bq/kg (Supporting information Table 1). This slight shift in water and dietary item ^{90}Sr activity concentration resulted in the prediction that water accounted for more than 80% of whole-body ^{90}Sr in *P. laevis*. The biodynamic model outputs suggest dissolved radiostrontium is a significant source of the radionuclide to the decapod crustacean, *P. laevis*. We believe this is the first report of the significance of the dissolved exposure pathway for

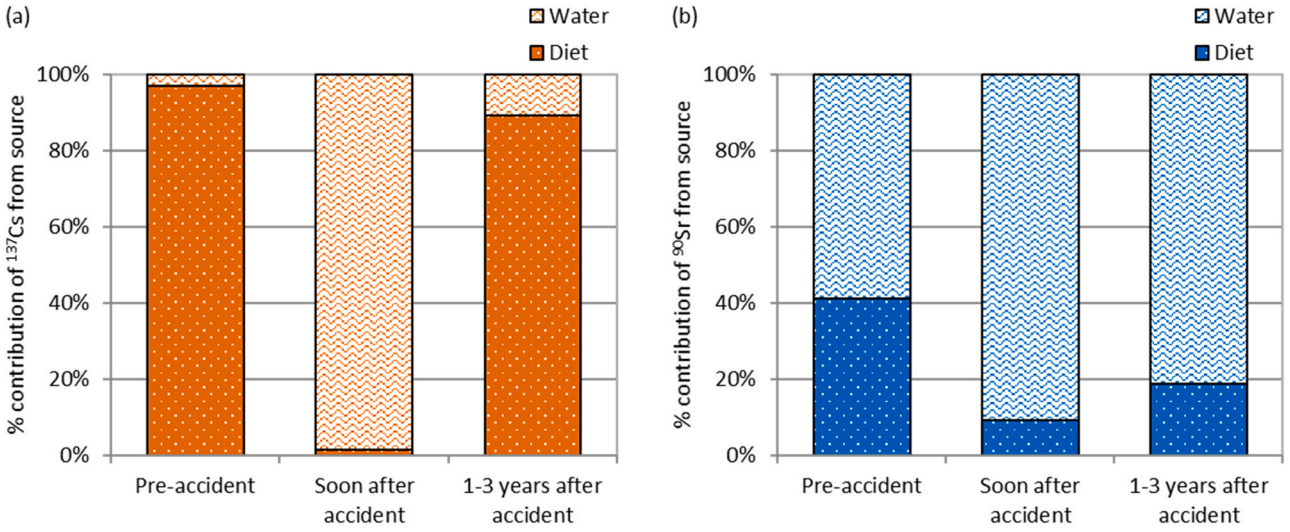

Fig. 7. Modelled relative contribution of water and dietary sources to whole-body (a) ^{137}Cs and (b) ^{90}Sr for a marine crab, theoretically exposed to radionuclides: pre-accident; soon after the accident (< 3 months); and 1–3 years after the accident based on data from 0.5 to 10 km from the FDNPP (see Supplemental Information for assumptions).

radiostrontium to decapod crustaceans.

4. Conclusion

The combination of live-animal radioisotope tracing with imaging from autoradiography and synchrotron XFM has allowed for an in-depth study of bioaccumulation kinetics and biodistribution of radiocaesium and radiostrontium in the mottled shore crab *P. laevis*. Radiocaesium and radiostrontium were readily accumulated from both water and diet. Exposure to radiolabelled sediment suggested the primary uptake pathway for ^{134}Cs was via solution from desorption of the radionuclide into the surrounding water. Future studies investigating exposure to radiolabelled sediment in the laboratory must be mindful of this occurrence, and therefore the potential issues extrapolating laboratory results to a field scenario.

Moulting occurred randomly by a few crabs during the long-term exposure (5 of 12 moulted). While data on moulting were few, ecdysis has a significant impact on both ^{134}Cs and ^{85}Sr bioaccumulation with Cs exhibiting a medium-term decrease and Sr exhibiting highly elevated increased uptake after moulting. These changes in radionuclide regulation kinetics are such that the concept of "equilibrium with surrounding solution" should not be assumed for similar moulting species. Future work should seek to understand and quantify the importance of moulting on radionuclide regulation within decapod crustaceans.

Following bioaccumulation, ^{134}Cs was internally translocated to extremity muscle tissue rapidly (within 6 h) while ^{85}Sr accumulated at the highest activity concentration in the gonad. Further work is required to understand the effects of long-term bioaccumulation of radiostrontium in the gonad of decapod crustaceans, especially with regards to potential dose impacts to that organ's function. Furthermore, accidental releases from nuclear facilities can result in substantial increases in dissolved ^{90}Sr concentrations as was experienced following the FDNPP accident, and understanding the consequences of these releases to marine invertebrates is crucial for ecosystem management.

Biodynamic modelling of radionuclides using pre- and post-accident monitoring data of water and benthic dietary items around the FDNPP confirmed dietary bioaccumulation pathways were most important for radiocaesium under non-accidental release conditions. However, the water pathway would likely dominate shortly after large releases of the radionuclide enter the aquatic environment. Dissolved radiostrontium sources were predicted to dominate the uptake pathways for *P. laevis*, accounting for 60–80% of whole-body activity concentration under non-accidental release scenarios and $>$ 90% shortly after large accident releases. Our findings highlight the importance of using laboratory-based biokinetic studies to understand organism responses to accidental releases of radionuclides to the aquatic environment.

CRediT authorship contribution statement

Tom Cresswell: Conceptualization, Methodology, Validation, Investigation, Formal analysis, Writing - Original Draft, Visualization, Supervision. **Emily Prentice:** Methodology, Validation, Investigation, Formal analysis, Writing - Review & Editing. **Nick Howell:** Methodology, Validation, Investigation, Writing - Review & Editing, Visualization. **Paul Callaghan:** Methodology, Validation, Investigation, Writing - Review & Editing. **Marc Metian:** Formal analysis, Writing - Review & Editing. **Mathew P. Johansen:** Conceptualization, Methodology, Formal analysis, Writing - Review & Editing, Visualization.

Declaration of Competing Interest

The authors declare that they have no known competing financial interests or personal relationships that could have appeared to influence the work reported in this paper.

Acknowledgements

The authors wish to thank the following ANSTO staff: Zoe Williams and An Nguyen for cryosectioning and autoradiography assistance; Henri Wong and Lida Mokhber-Shahin for assistance with ICP-MS and Gamma Spectrometry analysis respectively. Part of this research was undertaken on the XFM beamline at the Australian Synchrotron (ANSTO), Australia and the authors thank Daryl Howard for his assistance. On behalf of M.M., the IAEA is grateful to the Government of the Principality of Monaco for the support provided to its Environment Laboratories. This research formed part of the IAEA Coordinated Research Project, Applied Radioecological Tracers to Assess Coastal and Marine Ecosystem Health (K41019). This research did not receive any specific grant from funding agencies in the public, commercial, or not-for-profit sectors.

Appendix A. Supporting information

Supplementary data associated with this article can be found in the online version at doi:10.1016/j.jhazmat.2020.124453.

References

Aarkrog, A., Baxter, M.S., Bettencourt, A.O., Bojanowski, R., Bologa, A., Charmasson, S., Cunha, I., Delfanti, R., Duran, E., Holm, E., Jeffree, R., Livingston, H.D., Mahapanyawong, S., Nies, H., Osvath, I., Pingyu, L., Povinec, P.P., Sanchez, A., Smith, J.N., Swift, D., 1997. A comparison of doses from 137Cs and 210Po in marine food: A major international study. J. Environ. Radioact. 34 (1), 69–90. https://doi.org/10.1016/0265-931X(96)00005-7.

Bezhenar, R., Jung, K.T., Maderich, V., Willemsen, S., de With, G., Qiao, F., 2016. Transfer of radiocaesium from contaminated bottom sediments to marine organisms through benthic food chains in post-Fukushima and post-Chernobyl periods. Biogeosciences 13 (10), 3021–3034. https://doi.org/10.5194/bg-13-3021-2016.

Brown, J.E., Alfonso, B., Avila, R., Beresford, N.A., Copplestone, D., Hosseini, A., 2016. A new version of the ERICA tool to facilitate impact assessments of radioactivity on wild plants and animals. J. Environ. Radioact. 153, 141–148. https://doi.org/10.1016/j.jenvrad.2015.12.011.

Bryan, G.W., 1961. The accumulation of radioactive caesium in crabs. J. Mar. Biol. Assoc. U. K. 41 (03), 551–575. https://doi.org/10.1017/S0025315400016155.

Buesseler, K., Dai, M., Aoyama, M., Benitez-Nelson, C., Charmasson, S., Higley, K., Maderich, V., Masqué, P., Morris, P.J., Oughton, D., Smith, J.N., 2017. Fukushima Daiichi–derived radionuclides in the ocean: transport, fate, and impacts. Annu. Rev. Mar. Sci. 9 (1), 173–203. https://doi.org/10.1146/annurev-marine-010816-060733.

Caffrey, E.A., Higley, K.A., 2013. Creation of a voxel phantom of the ICRP reference crab. J. Environ. Radioact. 120, 14–18. https://doi.org/10.1016/j.jenvrad.2013.01.006.

Carroll, J., Boisson, F., Teyssie, J.L., King, S.E., Krosshavn, M., Carroll, M.L., Fowler, S. W., Povinec, P.P., Baxter, M.S., 1999. Distribution coefficients (Kd's) for use in risk assessment models of the Kara Sea. Appl. Radiat. Isot. 51 (1), 121–129. https://doi.org/10.1016/S0969-8043(98)00165-1.

Castrillejo, M., Casacuberta, N., Breier, C.F., Pike, S.M., Masqué, P., Buesseler, K.O., 2016. Reassessment of 90Sr, 137Cs, and 134Cs in the coast off Japan derived from the Fukushima Dai-ichi nuclear accident. Environ. Sci. Technol. 50 (1), 173–180. https://doi.org/10.1021/acs.est.5b03903.

Cresswell, T., Mazumder, D., Callaghan, P.D., Nguyen, A., Corry, M., Simpson, S.L., 2017a. Metal transfer among organs following short- and long-term exposures using autoradiography: cadmium bioaccumulation by the freshwater prawn *Macrobrachium australiense*. Environ. Sci. Technol. 51 (7), 4054–4060. https://doi.org/10.1021/acs.est.6b06471.

Cresswell, T., Metian, M., Golding, L.A., Wood, M.D., 2017b. Aquatic live animal radiotracing studies for ecotoxicological applications: addressing fundamental methodological deficiencies. J. Environ. Radioact. 178–179, 435–460. https://doi.org/10.1016/j.jenvrad.2017.05.017.

Cresswell, T., Simpson, S.L., Mazumder, D., Callaghan, P.D., Nguyen, A.P., 2015. Bioaccumulation kinetics and organ distribution of cadmium and zinc in the freshwater decapod crustacean *Macrobrachium australiense*. Environ. Sci. Technol. 49, 1182–1189. https://doi.org/10.1021/es505254w.

Cresswell, T., Simpson, S.L., Smith, R.E.W., Nugegoda, D., Mazumder, D., Twining, J., 2014a. Bioaccumulation and retention kinetics of cadmium in the freshwater decapod *Macrobrachium australiense*. Aquat. Toxicol. 148, 174–183. https://doi.org/10.1016/j.aquatox.2014.01.006.

Cresswell, T., Smith, R.E.W., Nugegoda, D., Simpson, S.L., 2014b. Comparing trace metal bioaccumulation characteristics of three freshwater decapods of the genus *Macrobrachium*. Aquat. Toxicol. 152, 256–263. https://doi.org/10.1016/j.aquatox.2014.04.015.

Dutton, J., Fisher, N.S., 2014. Modeling metal bioaccumulation and tissue distribution in killifish (Fundulus heteroclitus) in three contaminated estuaries. Environ. Toxicol. Chem. 33 (1), 89–101. https://doi.org/10.1002/etc.2392.

Fiévet, B., Bailly-du-Bois, P., Laguionie, P., Morillon, M., Arnaud, M., Cunin, P., 2017. A dual pathways transfer model to account for changes in the radioactive caesium

level in demersal and pelagic fish after the Fukushima Daï-ichi nuclear power plant accident. PloS One 12 (3), e0172442. https://doi.org/10.1371/journal.pone.0172442.
Harmelin-Vivien, M., Bodiguel, X., Charmasson, S., Loizeau, V., Mellon-Duval, C., Tronczyński, J., Cossa, D., 2012. Differential biomagnification of PCB, PBDE, Hg and Radiocesium in the food web of the European hake from the NW Mediterranean. Mar. Pollut. Bull. 64 (5), 974–983. https://doi.org/10.1016/j.marpolbul.2012.02.014.
Howard, B.J., Beresford, N.A., Copplestone, D., Telleria, D., Proehl, G., Fesenko, S., Jeffree, R.A., Yankovich, T.L., Brown, J.E., Higley, K., Johansen, M.P., Mulye, H., Vandenhove, H., Gashchak, S., Wood, M.D., Takata, H., Andersson, P., Dale, P., Ryan, J., Bollhöfer, A., Doering, C., Barnett, C.L., Wells, C., 2013. The IAEA handbook on radionuclide transfer to wildlife. J. Environ. Radioact. 121 (Supplement C), 55–74. https://doi.org/10.1016/j.jenvrad.2012.01.027.
IAEA,2004. Sediment Distribution Coefficients and Concentration Factors for Biota in the Marine Environment, Technical Report Series No. 422. Vienna.
ICRP, 2008. Environmental protection - the concept and use of reference animals and plants. ICRP Publication 108. Ann. ICRP 38 (4–6).
Jeffree, R.A., Oberhansli, F., Teyssie, J.-L., Fowler, S.W., 2015. Maternal transfer of anthropogenic radionuclides to eggs in a small shark. J. Environ. Radioact. 147, 43–50. https://doi.org/10.1016/j.jenvrad.2015.05.009.
Johansen, M.P., Cresswell, T., Davis, J., Howard, D.L., Howell, N., Prentice, E., 2019. Biofilm-enhanced adsorption of strong and weak cations onto different microplastic sample types: use of spectroscopy, microscopy and radiotracer methods. Water Res. 158, 392–400. https://doi.org/10.1016/j.watres.2019.04.029.
Johansen, M.P., Ruedig, E., Tagami, K., Uchida, S., Higley, K., Beresford, N.A., 2015. Radiological dose rates to marine fish from the Fukushima Daiichi accident: the first three years ccross the North Pacific. Environ. Sci. Technol. 49 (3), 1277–1285. https://doi.org/10.1021/es505064d.
Kasamatsu, F., Ishikawa, Y., 1997. Natural variation of radionuclide 137Cs concentration in marine organisms with special reference to the effect of food habits and trophic level. Mar. Ecol. Prog. Ser. 160, 109–120. https://doi.org/10.3354/meps160109.
King, C.K., Dowse, M.C., Simpson, S.L., Jolley, D.F., 2004. An assessment of five australian polychaetes and bivalves for use in whole-sediment toxicity tests: toxicity and accumulation of copper and zinc from water and sediment. Arch. Environ. Contam. Toxicol. 47 (3), 314–323. https://doi.org/10.1007/s00244-004-3122-1.
Kusakabe, M., Oikawa, S., Takata, H., Misonoo, J., 2013. Spatiotemporal distributions of Fukushima-derived radionuclides in nearby marine surface sediments. Biogeosciences 10 (7), 5019–5030. https://doi.org/10.5194/bg-10-5019-2013.
Landrum, P.F., Lydy, M.J., Lee, H., 1992. Toxicokinetics in aquatic systems: model comparisons and use in hazard assessment. Environ. Toxicol. Chem. 11 (12), 1709–1725. https://doi.org/10.1002/etc.5620111205.
Lee, J.S., Lee, B.G., 2005. Effects of salinity, temperature and food type on the uptake and elimination rates of cd, cr, and zn in the asiatic clamcorbicula fluminea. Ocean Sci. J. 40 (2), 79–89. https://doi.org/10.1007/BF03028588.
Lee, P.-F., Wang, J.-J., Huang, J.-C., 2013. The accumulation study of 90Sr in fish from a fishpond of northern Taiwan. Appl. Radiat. Isot. 81, 321–324. https://doi.org/10.1016/j.apradiso.2013.03.010.
Mathews, T., Fisher, N.S., 2008. Trophic transfer of seven trace metals in a four-step marine food chain. Mar. Ecol. Prog. Ser. 367, 23–33.
Mathews, T., Fisher, N.S., 2009. Dominance of dietary intake of metals in marine elasmobranch and teleost fish. Sci. Total Environ. 407 (18), 5156–5161. https://doi.org/10.1016/j.scitotenv.2009.06.003.
Mazumder, D., Saintilan, N., 2010. Mangrove leaves are not an important source of dietary carbon and nitrogen for crabs in temperate Australian Mangroves. Wetlands 30 (2), 375–380. https://doi.org/10.1007/s13157-010-0021-2.
Metian, M., Pouil, S., Fowler, S.W., 2019. Radiocesium accumulation in aquatic organisms: a global synthesis from an experimentalist's perspective. J. Environ. Radioact. 198, 147–158. https://doi.org/10.1016/j.jenvrad.2018.11.013.
Metian, M., Pouil, S., Hédouin, L., Oberhänsli, F., Teyssié, J.-L., Bustamante, P., Warnau, M., 2016. Differential bioaccumulation of ^{134}Cs in tropical marine organisms and the relative importance of exposure pathways. J. Environ. Radioact. 152, 127–135. https://doi.org/10.1016/j.jenvrad.2015.11.012.
Mohapatra, A., Rautray, T.R., Patra, A.K., Vijayan, V., Mohanty, R.K., 2009. Trace element-based food value evaluation in soft and hard shelled mud crabs. Food Chem. Toxicol.: Int. J. Publ. Br. Ind. Biol. Res. Assoc. 47 (11), 2730–2734. https://doi.org/10.1016/j.fct.2009.07.037.
Nagaya, Y., Nakamura, K., Saiki, M., 1971. Strontium concentrations and strontium-chlorinity ratios in sea water of the North Pacific and the adjacent seas of Japan. J. Oceanogr. Soc. Jpn. 27 (1), 20–26. https://doi.org/10.1007/BF02109311.
Pan, K., Wang, W.-X., 2016. Radiocesium uptake, trophic transfer, and exposure in three estuarine fish with contrasting feeding habits. Chemosphere 163, 499–507. https://doi.org/10.1016/j.chemosphere.2016.08.066.
Pinder, J.E., Hinton, T.G., Taylor, B.E., Whicker, F.W., 2011. Cesium accumulation by aquatic organisms at different trophic levels following an experimental release into a small reservoir. J. Environ. Radioact. 102 (3), 283–293. https://doi.org/10.1016/j.jenvrad.2010.12.003.
Pouil, S., Teyssié, J.-L., Fowler, S.W., Metian, M., Warnau, M., 2018. Interspecific comparison of radiocesium trophic transfer in two tropical fish species. J. Environ. Radioact. 189, 261–265. https://doi.org/10.1016/j.jenvrad.2018.04.008.
R Core Team, 2020. R: A Language and Environment for Statistical Computing. R Foundation for Statistical Computing, Vienna, Austria. ⟨http://www.R-project.org/⟩.
Rowan, D.J., 2013a. Bioaccumulation factors and the steady state assumption for cesium isotopes in aquatic foodwebs near nuclear facilities. J. Environ. Radioact. 121, 2–11. https://doi.org/10.1016/j.jenvrad.2012.03.008.
Rowan, D.J., 2013b. Bioaccumulation factors and the steady state assumption for cesium isotopes in aquatic foodwebs near nuclear facilities. J. Environ. Radioact. 121 (0), 2–11. https://doi.org/10.1016/j.jenvrad.2012.03.008.
Rowan, J.R., Rasmussen, J.B., 1994. Bioaccumulation of radiocesium by fish: the influence of physicochemical factors and trophic structure. Can. J. Fish. Aquat. Sci. 51, 2388–2410.
Ruedig, E., Beresford, N.A., Gomez Fernandez, M.E., Higley, K., 2015. A comparison of the ellipsoidal and voxelized dosimetric methodologies for internal, heterogeneous radionuclide sources. J. Environ. Radioact. 140 (0), 70–77. https://doi.org/10.1016/j.jenvrad.2014.11.004.
Ryan, C.G., Kirkham, R., Hough, R.M., Moorhead, G., Siddons, D.P., de Jonge, M.D., Paterson, D.J., De Geronimo, G., Howard, D.L., Cleverley, J.S., 2010. Elemental X-ray imaging using the Maia detector array: the benefits and challenges of large solid-angle. Nucl. Instrum. Methods Phys. Res. Sect. A: Accel. Spectrom. Detect. Assoc. Equip. 619 (1), 37–43. https://doi.org/10.1016/j.nima.2009.11.035.
Schurr, J.M., Stamper, M.N., 1962. Model for the accumulation of strontium and calcium by recently molted crayfish (*Cambarus longulus longerostris ort.*). Limnol. Oceanogr. 7 (4), 474–477. https://doi.org/10.4319/lo.1962.7.4.0474.
Sezer, N., Belivermiş, M., Kılıç, Ö., Topcuoğlu, S., Çotuk, Y., 2014. Biokinetics of radiocesium in shrimp (Palaemon adspersus): seawater and food exposures. J. Environ. Radioact. 132 (0), 15–20. https://doi.org/10.1016/j.jenvrad.2014.01.014.
Sohtome, T., Wada, T., Mizuno, T., Nemoto, Y., Igarashi, S., Nishimune, A., Aono, T., Ito, Y., Kanda, J., Ishimaru, T., 2014. Radiological impact of TEPCO's Fukushima Dai-ichi nuclear power plant accident on invertebrates in the coastal benthic food web. J. Environ. Radioact. 138 (0), 106–115. https://doi.org/10.1016/j.jenvrad.2014.08.008.
Takata, H., Johansen, M.P., Kusakabe, M., Ikenoue, T., Yokota, M., Takaku, H., 2019. A 30-year record reveals re-equilibration rates of 137Cs in marine biota after the Fukushima Dai-ichi nuclear power plant accident: concentration ratios in pre- and post-event conditions. Sci. Total Environ. 675, 694–704. https://doi.org/10.1016/j.scitotenv.2019.04.015.
Takata, H., Tagami, K., Aono, T., Uchida, S., 2014. Distribution coefficients (Kd) of strontium and significance of oxides and organic matter in controlling its partitioning in coastal regions of Japan. Sci. Total Environ. 490, 979–986. https://doi.org/10.1016/j.scitotenv.2014.05.101.
Tipping, E., 1994. WHAM - a chemical-equilibrium model and computer code for waters, sediments, and soils incorporating a discrete site electrostatic model of ion-binding by humic substances. Comput. Geosci. 20 (6), 973–1023. https://doi.org/10.1016/0098-3004(94)90038-8.
Ulanovsky, A., Prohl, G., Gomez-Ros, J.M., 2008. Methods for calculating dose conversion coefficients for terrestrial and aquatic biota. J. Environ. Radioact. 99 (9), 1440–1448. https://doi.org/10.1016/j.jenvrad.2008.01.010.
Wada, T., Fujita, T., Nemoto, Y., Shimamura, S., Mizuno, T., Sohtome, T., Kamiyama, K., Narita, K., Watanabe, M., Hatta, N., Ogata, Y., Morita, T., Igarashi, S., 2016. Effects of the nuclear disaster on marine products in Fukushima: an update after five years. J. Environ. Radioact. 164, 312–324. https://doi.org/10.1016/j.jenvrad.2016.06.028.
Wang, C., Baumann, Z., Madigan, D.J., Fisher, N.S., 2016a. Contaminated marine sediments as a source of cesium radioisotopes for benthic fauna near Fukushima. Environ. Sci. Technol. 50 (19), 10448–10455. https://doi.org/10.1021/acs.est.6b02984.
Wang, C.Y., Baumann, Z., Madigan, D.J., Fisher, N.S., 2016b. Contaminated marine sediments as a source of cesium radioisotopes for benthic fauna near Fukushima. Environ. Sci. Technol. 50 (19), 10448–10455. https://doi.org/10.1021/acs.est.6b02984.
Wang, W.X., Ke, C.H., 2002. Dominance of dietary intake of cadmium and zinc by two marine predatory gastropods. Aquat. Toxicol. 56 (3), 153–165. https://doi.org/10.1016/s0166-445x(01)00205-3.
Wang, W.X., Wong S.K., R., 2003. Bioaccumulation kinetics and exposure pathways of inorganic mercury and methylmercury in a marine fish, the sweetlips Plectorhinchus gibbosus. Mar. Ecol. Prog. Ser. 261, 257–268. https://doi.org/10.3354/meps261257.
Zhao, X., Wang, W.-X., Yu, K.N., K. S. Lam, P., 2001. Biomagnification of radiocesium in a marine piscivorous fish. Mar. Ecol. Prog. Ser. 222, 227–237.